AGU PUBLICATIONS

Water Resources Research

RESEARCH ARTICLE
10.1002/2016WR020254

Evapotranspiration of urban landscapes in Los Angeles, California at the municipal scale

E. Litvak[1], K. F. Manago[2], T. S. Hogue[2], and D. E. Pataki[1]

[1]Department of Biology, University of Utah, Salt Lake City, Utah, USA, [2]Civil and Environmental Engineering Department, Colorado School of Mines, Illinois, Colorado, USA

Key Points:
- Evapotranspiration from irrigated landscapes in Los Angeles was close to reference evapotranspiration
- Turfgrass was responsible for 70% of evapotranspiration from vegetated areas
- Evapotranspiration from total land area (vegetated and nonvegetated) was linearly correlated with median household income

Supporting Information:
- Supporting Information S1
- Table S1

Correspondence to:
E. Litvak,
elitvak@uci.edu

Citation:
Litvak, E., K. F. Manago, T. S. Hogue, and D. E. Pataki (2017), Evapotranspiration of urban landscapes in Los Angeles, California at the municipal scale, *Water Resour. Res.*, *53*, 4236–4252, doi:10.1002/2016WR020254.

Received 9 DEC 2016
Accepted 27 APR 2017
Published online 24 MAY 2017

Abstract Evapotranspiration (*ET*), an essential process in biosphere-atmosphere interactions, is highly uncertain in cities that maintain cultivated and irrigated landscapes. We estimated *ET* of irrigated landscapes in Los Angeles by combining empirical models of turfgrass *ET* and tree transpiration derived from in situ measurements with previously developed remotely sensed estimates of vegetation cover and ground-based vegetation surveys. We modeled irrigated landscapes as a two-component system comprised of trees and turfgrass to assess annual and spatial patterns of *ET*. Annual *ET* from vegetated landscapes (ET_{veg}) was 1110 ± 53 mm/yr and *ET* from the whole city (vegetated and nonvegetated areas, ET_{land}) was three times smaller, reflecting the fractional vegetation cover. With the exception of May and June, monthly ET_{land} was significantly higher than predicted by the North American Land Data Assimilation System. ET_{veg} was close to potential *ET*, indicating abundant irrigation inputs. Monthly averaged ET_{veg} varied from 1.5 ± 0.1 mm/d (December) to 4.3 ± 0.2 mm/d (June). Turfgrass was responsible for ~70% of ET_{veg}. For trees, angiosperm species (71% of all trees) contributed over 90% to total tree transpiration, while coniferous and palm species made very small contributions. ET_{land} was linearly correlated with median household income across the city, confirming the importance of social factors in determining spatial distribution of urban vegetation. These estimates have important implications for constraining the municipal water budget of Los Angeles and improving regional-scale hydrologic models, as well as for developing water-saving practices. The methodology used in this study is also transferable to other semiarid regions for quantification of urban landscape *ET*.

1. Introduction

Urban evapotranspiration (*ET*) is an essential component of water and energy budgets of vegetated cities, yet it is still highly uncertain [*Pittenger and Shaw*, 2007, 2010; *Pataki et al*., 2011a; *Shields and Tague*, 2012; *Sun et al*., 2012; *Nouri et al*., 2013]. Heterogeneous urban land cover is a patchwork of vegetation and built structures, which results in complex patterns of *ET* [*Grimmond et al*., 1996; *Grimmond and Oke*, 1999; *Offerle et al*., 2006; *Anderson and Vivoni*, 2016]. In addition, there is a paucity of in situ measurements of *ET* in virtually all types of urban land cover [*Boegh et al*., 2009; *Hart et al*., 2009; *Pittenger and Shaw*, 2010; *Pataki et al*., 2011b; *Nouri et al*., 2013]. In dry regions, urban *ET* may be much larger than the surrounding natural ecosystem and therefore plays a significant role in local hydrologic fluxes [*Grimmond and Oke*, 1999]. Measuring and modeling *ET* is particularly challenging in urban regions with diverse and nonnative plant composition [*Pataki et al*., 2011b; *Peters et al*., 2011].

The city of Los Angeles has more than 6 million trees, most of which are nonnative and originate from mesic environments in multiple geographic regions and continents [*Dwyer et al*., 2000; *Clarke et al*., 2013; *Pataki et al*., 2013]. In natural environments, *ET* in southern California is primarily controlled by groundwater availability and the amount and timing of precipitation events [*Duell*, 1991; *de Vries and Simmers*, 2002; *Hamlet et al*., 2007; *Goulden et al*., 2012]. In irrigated urban areas with diverse plant composition such as Los Angeles, surface soil moisture may be nonlimiting, such that *ET* is largely controlled by stomatal responses of landscape plants to environmental conditions in the presence of advection [*Grimmond and Oke*, 1999]. The combination of moist, irrigated soil and dry air often exposes cultivated plants to conditions beyond the range of their natural habitats, resulting in a variety of transpiration patterns [*Litvak et al*., 2011, 2012; *Pataki et al*., 2011b]. For example, the majority of trees in Los Angeles are imported from mesic temperate and tropical regions, which are more humid than the local environment [*Nowak et al*., 2010; *Avolio et al*.,

2015; *Jenerette et al*., 2016]. In a study of 14 tree species in the Los Angeles Metropolitan area, transpiration of urban trees measured in situ varied from 3 to 177 kg d^{-1} per individual tree [*Pataki et al*., 2011b]. Such a wide range of values makes it difficult to estimate urban forest *ET* at large spatial scales. On a plot scale, transpiration of single-species tree stands with a fixed reference density of 100 trees ha^{-1}, which is common in urban landscapes, varied from 0.1 to 2.6 mm d^{-1} in a previous study in Los Angeles [*Litvak et al*., 2017]. In contrast, *ET* of irrigated turfgrass lawns in the Los Angeles Metropolitan area reached 6 mm d^{-1} during regular summertime conditions, and 10 mm d^{-1} during extremely dry weather [*Litvak et al*., 2014; *Litvak and Pataki*, 2016].

ET of relatively large areas, such as the city of Los Angeles, are currently estimated by scaling regional reference *ET* measurements [*Hart et al*., 2009; *Spano et al*., 2009; *Aminzadeh and Or*, 2017] or by coupling remotely sensed satellite products (namely, vegetation indices and land surface temperature) with either the Penman-Monteith equation or surface energy balance models [*Boegh et al*., 2009; *Zhang et al*., 2010; *Mu et al*., 2011; *Vahmani and Hogue*, 2014a,b,; *Wang et al*., 2016a]. However, high quality, cloud-free satellite data are often unavailable [*Nishida et al*., 2003; *Long and Singh*, 2013; *Long et al*., 2014]. Moreover, the ground-based meteorological data required by most *ET* algorithms may not be available at the fine spatial resolution that would match the resolution achieved by satellite remote sensing [*Yang et al*., 2013]. These factors result in large uncertainties in satellite-based *ET* estimates. Large-scale *ET* is also obtained from micrometeorological measurements, particularly eddy covariance [*Grimmond and Oke*, 1999; *Offerle et al*., 2006; *Balogun et al*., 2009; *Peters et al*., 2011; *Nordbo et al*., 2012; *Anderson and Vivoni*, 2016; *Xie et al*., 2016]. However, these estimates have very limited spatial coverage in urban centers, as well as large uncertainties due to landscape heterogeneity in cities, and are not able to discern the contributions of particular plant types [*Roth*, 2000; *Schmid*, 2002].

Among currently available large-scale *ET* estimates, the Land Data Assimilation System (LDAS; ldas.gsfc.nasa.gov) is commonly used [*Long et al*., 2014]. LDAS is a set of land surface models (LSM) of different origins forced with in situ and remotely sensed observations and output from numerical prediction models [*Kumar et al*., 2006]. There are four North American LDAS (NLDAS) models: Mosaic [*Koster and Suarez*, 1994], VIC [*Liang et al*., 1994], Noah [*Chen et al*., 1996], and SAC [*Mitchell et al*. 2004; ldas.gsfc.nasa.gov/nldas]. These models involve different soil-vegetation-atmosphere transfer schemes, with Mosaic and VIC incorporating subgrid vegetation composition, Noah only taking into account the dominating vegetation type within each grid, and SAC not explicitly including vegetation (https://ldas.gsfc.nasa.gov/nldas/NLDAS2model.php) [*Mitchell et al*., 2004]. Monthly *ET* predictions with 1/8° (∼14 km) resolution are available from these NLDAS models.

The goal of the current study was to estimate *ET* of the vegetated landscape in Los Angeles by upscaling in situ measurements and comparing these estimates to predictions from LDAS. We developed a methodology for upscaling in situ tree transpiration measured in 2007 and 2008, as well as turfgrass *ET* measured in 2010. Previous studies have shown that turfgrass *ET* is largely controlled by incoming solar radiation, and strongly influenced by shading from trees and other structures [*Feldhake et al*., 1983; *Shashua-Bar et al*., 2009; *Litvak et al*., 2014]. Tree transpiration is dependent on species, planting density, and tree dimensions, along with environmental parameters [*Litvak and Pataki*, 2016; *Litvak et al*., 2017]. Here we combine empirical models derived from in situ measurements, assessments of canopy cover based on high-resolution remote sensing, ground surveys of plant species composition, and weather parameters for the years 2007–2008, to obtain citywide estimates of *ET*. The following questions were addressed: (1) what is the total *ET* of lawns and forested landscapes in Los Angeles and how well does it correspond to LSM estimates? (2) What are relative contributions of turfgrass and trees to *ET*? (3) How variable is *ET* spatially, considering varying canopy and lawn cover throughout the city?

Specifically, we examined the spatial *ET* patterns in relation to median household income (MHI). While there is certainly not likely to be a direct influence of MHI on *ET*, affluent neighborhoods in Los Angeles were shown to have higher tree cover and lower surface temperatures than less affluent neighborhoods [*Clarke et al*., 2013]. Therefore, we expected *ET* to be consistently higher in more affluent parts of the city.

This study provides the first municipal scale estimates of *ET* based on in situ measurements, differentiated by plant types and composition. Such estimates are critical for constraining urban water and energy budgets, and ultimately in designing interventions that are beneficial for water conservation. Accurate estimates

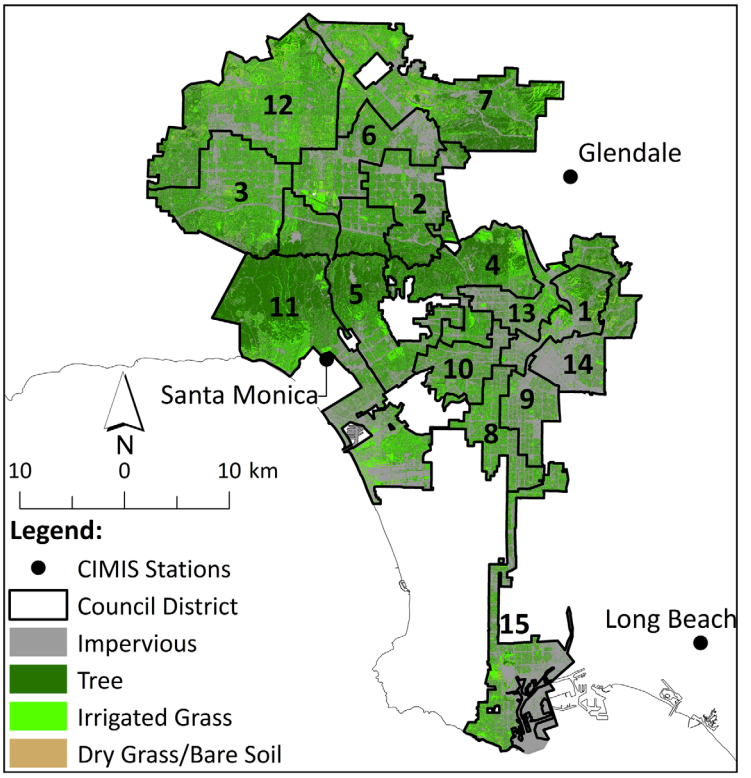

Figure 1. The City of Los Angeles, its council districts, and the nearest California Irrigation Management Information System (CIMIS) weather stations operated in 2007–2008 (black circles; CIMIS station #99—Santa Monica, #133—Glendale, and #174—Long Beach).

of *ET* resolved by plant type are particularly important in California, which is currently experiencing an unprecedented drought. The methodological approach developed in this study may also be used for estimating *ET* in other urbanized areas.

2. Methods

2.1. Study Area

The City of Los Angeles is the second largest city in the United States and the core of one of the most populous metropolitan areas in the world (U.S. Census Bureau, www.census.gov). The City is situated in a coastal plain and surrounded by mountain ranges. The climate is Mediterranean, with mean annual temperatures of 17.0–18.3°C and annual precipitation of 326–377 mm/yr that mainly occurs in winter (Western Regional Climate Center, www.wrcc.dri.edu). Los Angeles is composed of 15 council districts (Figure 1), which have been used in previous studies that have characterized tree and turfgrass cover using remote sensing data [*McPherson et al*., 2008, 2011].

2.2. Turfgrass and Tree Cover

Turfgrass and tree cover for Los Angeles were obtained from the most recent and precise land cover database that includes four land cover types: irrigated grass, tree canopy cover, bare soil, and impervious surface, obtained from the analysis of satellite imagery at 0.6 m resolution combined with GIS layers and aerial photography [*McPherson et al*., 2008, 2011]. According to this data set, turfgrass not covered by tree canopies accounts for approximately 12,629 ha and tree canopy cover (A_{TCC}; includes both tree and shrub covers) accounts for 21,243 ha [*McPherson et al*., 2008, 2011]. Thus, cumulative vegetation cover in Los Angeles (A_{veg}) is approximately 33,872 ha.

We estimated total turfgrass area in Los Angeles as the sum of turfgrass covered by tree canopies and turfgrass not covered by tree canopies. As a first approximation, we assumed that all areas below tree canopies were covered by turfgrass [*McPherson et al*., 2008]. Then, the total turfgrass area is equal to A_{veg}, with fractional tree canopy cover above turfgrass $A_{TCC}/A_{veg} \approx 0.627$.

The approximate number of trees in Los Angeles (N_{LA}; calculated with an assumption that all trees have similar canopy areas) is 10,800,000 [*McPherson et al*., 2008, 2011]. Therefore, the density of urban trees on A_{veg} (d) is

$$d = \frac{N_{LA}}{A_{veg}} = 319 \text{ trees ha}^{-1} \quad (1)$$

Nowak et al. [2010] listed 140 tree species with estimated numbers of trees (N_i) and average diameter at breast height (*DBH*) for each species. According to *Nowak et al*. [2010], the Los Angeles urban forest consists of 71% flowering (angiosperm) trees, 15% coniferous (gymnosperm) trees, 11% palm trees, and 3% others

Table 1. List of Abbreviations

A_S (cm^2)	Sapwood area
A_{veg} (ha)	Cumulative vegetation cover (includes turfgrass and tree canopies)
A_{land} (ha)	Total land area (vegetated + nonvegetated)
A_{LDR} (ha)	Cumulative area of low-density residential lands
A_{TCC} (ha)	Tree canopy cover
CIMIS	California Irrigation Management Information System
D (kPa)	Vapor pressure deficit of the air
d (trees ha^{-1})	Density of trees on A_{veg}
d_i (trees ha^{-1})	Density of each tree species on A_{veg}
DBH (cm)	Diameter of trees at breast height
E_{con} (mm d^{-1})	Transpiration of coniferous (gymnosperm) trees from a cumulative vegetated area
E_{fl} (mm d^{-1})	Transpiration of flowering (angiosperm) trees from a cumulative vegetated area
E_{palms} (mm d^{-1})	Transpiration of palm trees from a cumulative vegetated area
E_{Trees} (mm d^{-1})	Tree transpiration from a cumulative vegetated area
ET_{land} (mm d^{-1})	Landscape transpiration from a total land area
ET_{veg} (mm d^{-1})	Landscape transpiration from a cumulative vegetated area
ET_0 (mm d^{-1})	Reference evapotranspiration
ET_{Grass} (mm d^{-1})	Evapotranspiration of turfgrass
I_0 (W m^{-2})	Incoming solar radiation
k_{mc}	Microclimate coefficient
MHI ($)	Median household income
N	Number of trees
N_{LA}	Total number of trees in Los Angeles
x (km)	Distance from the coast

(such as tree ferns and cycads, supporting information Table S1). Similar to *d*, we calculated the density of each species (*i*) on A_{veg} (d_i):

$$d_i = \frac{N_i}{A_{veg}} \tag{2}$$

2.3. The Model of Turfgrass *ET*

In situ measurements in the Los Angeles Metropolitan area showed that turfgrass *ET* (ET_{Grass}) did not tend to respond to decreasing soil moisture between irrigation events, and was therefore not commonly limited by soil water content [*Litvak et al.*, 2014; *Litvak and Pataki*, 2016]. Under water-unlimiting conditions, ET_{Grass} is determined by radiative and atmospheric factors, rather than physiological attributes of turfgrass [*Carrow et al.*, 1990]. Accordingly, previous in situ measurements in the Los Angeles Metropolitan area revealed similar ET_{Grass} of cool-season and warm-season grasses [*Bijoor et al.*, 2014; *Litvak et al.*, 2014; *Litvak and Pataki*, 2016].

To model ET_{Grass}, we used equations obtained from in situ measurements of lawns with different turfgrass composition and fractional A_{TCC} in the Los Angeles Metropolitan area [*Litvak and Pataki*, 2016]:

$$ET_{Grass} = k_{mc} ET_0, \tag{3}$$

$$k_{mc} = a - b\frac{A_{TCC}}{A_{veg}} \tag{4}$$

Here ET_0 is *ET* from a reference surface of irrigated turfgrass, k_{mc} is a "microclimate coefficient," and $a = 0.90 \pm 0.09$ and $b = 0.35 \pm 0.13$ are fixed model parameters [*Litvak and Pataki*, 2016]. $A_{TCC}/A_{veg} = 0.627$ for the entire city and varied across the council districts.

2.4. The Model of Tree Transpiration

We calculated urban forest transpiration from the cumulative vegetation area (E_{Trees}, mm d^{-1}) as the sum of the contributions from each species of flowering (angiosperm) trees (E_{fl}), coniferous (gymnosperm) trees (E_{con}) and palm trees (E_{palms}):

$$E_{Trees} = \sum E_{fl(i)} + \sum E_{con(i)} + E_{palms}. \tag{5}$$

We estimated E_{fl} and E_{con} using an empirical model obtained from in situ measurements of irrigated urban trees in the Los Angeles metropolitan area [*Litvak et al.*, 2017]:

$$E_{fl(i)} = 1.2\times10^{-6} d_i A_{S(i)} (5.5 + 2.3\ln D + 0.02 I_0), \tag{6a}$$

$$E_{con(i)} = 4.0\times10^{-7} d_i A_{S(i)} (5.5 + 2.3\ln D + 0.02 I_0), \tag{6b}$$

where $A_{S(i)}$ (cm^2) is the average sapwood area of each species, *D* (kPa) is the vapor pressure deficit of the air, and I_0 (W m^{-2}) is incoming solar radiation. Neither E_{fl} nor E_{con} depends on soil moisture, suggesting that these irrigated trees generally receive a nonlimiting water supply [*McCarthy and Pataki*, 2010; *Litvak et al.*, 2011, 2012, 2017].

To estimate sapwood area of Los Angeles urban trees, we established empirical relationships between A_S and *DBH* using the dimensions of 115 urban trees (14 species) measured in the Los Angeles region. We

used SigmaPlot (Version 10, Systat Software Inc., Chicago, IL, USA) for curve fitting. For species with *DBH* smaller than our measured minimum (8.7 cm), we assumed that

$$A_S \approx \pi\left(\frac{DBH}{2}\right)^2. \tag{7}$$

The physiology of palm trees is very different from both angiosperms and gymnosperms; in particular, they do not have distinct sapwood. We estimated E_{palms} based on in situ measurements of Mexican fan palm transpiration in the Los Angeles Arboretum and Botanic Gardens [*Renninger et al*., 2009]. *Renninger et al*. [2009] found that transpiration of individual palm trees with leaf areas of 0.79–1.74 m^2 varied from 0.5 to 1.7 kg d^{-1} m^{-2}. Therefore, transpiration of individual Mexican fan palms was 0.4–3.0 kg d^{-1}, which is equivalent to 0.004–0.03 mm d^{-1} for a stand with a planting density of 100 trees ha^{-1} (to convert the units to mm d^{-1}, we multiplied individual tree transpiration in kg d^{-1} by 0.01 trees m^{-2}, which is the metric equivalent of 100 trees ha^{-1}, and divided by the density of water). These values are extremely low compared to transpiration of other tree species [*Pittenger et al*., 2009; *Pataki et al*., 2011b]. Because time series of palm transpiration in Los Angeles are not available, we assumed that E_{palms} is the same year round and

$$0.004\frac{d_{palms}}{100} \le E_{palms} \le 0.03\frac{d_{palms}}{100}, \tag{8}$$

where d_{palms} is the density of all palm trees on tree canopy covered area of the Los Angeles landscape.

2.5. Landscape *ET*

We calculated landscape *ET* from the cumulative vegetation area (ET_{veg}) as the sum of contributions from trees and turfgrass, which are the major components of the Los Angeles vegetated landscape:

$$ET_{veg} = ET_{Grass} + ET_{Trees} \approx ET_{Grass} + E_{Trees}. \tag{9}$$

We substituted E_{Trees} for *ET* from tree canopies (ET_{Trees}) because of the low and infrequent rainfall in the Los Angeles metropolitan area, where tree canopies stay dry most of the time. Irrigation, the dominant water input in this area, is applied at the ground level and does not wet tree canopies. Low (375 mm/yr) and infrequent (36 rain days/yr) rainfall mainly happens in winter (averages for 1877–2016; Western Regional Climate Center, www.wrcc.dri.edu). However, evaporation is lower in winter than in the other seasons due to reduced solar radiation and air temperatures. Tree canopy interception is also reduced in winter when deciduous trees that comprise ~22% of Los Angeles urban forest [*Nowak et al*., 2010] are leafless. Therefore, in this Mediterranean-type, irrigation-sustained environment, evaporation from tree canopies may be considered negligible compared to tree transpiration.

Because deciduous trees were leafless during December and January, we assumed they had zero transpiration during these months. We calculated ET_{veg} for each council district using tree and turfgrass canopy covers reported by *McPherson et al*. [2011] and environmental data as described below. The model we used to estimate ET_{Grass} (equations (3) and (4)) does not depend on species composition, but the model of E_{Trees} (equations (5) and (6)) depends on the proportion of flowering, coniferous and palm trees in the landscape. Because of the lack of the data on tree species composition for each council district, we assumed a uniform species composition across the whole city.

We calculated landscape *ET* from the total land area of each council district (A_{land}) as

$$ET_{land} = ET_{veg}\frac{A_{veg}}{A_{land}} + E_{non\text{-}veg}\frac{A_{non\text{-}veg}}{A_{land}} \approx ET_{veg}\frac{A_{veg}}{A_{land}}, \tag{10}$$

and ET_{veg} and ET_{land} of the entire city of Los Angeles as the weighted sum of all the 15 council districts. Here $E_{non\text{-}veg}$ is the evaporation from nonvegetated areas such as bare soil and impervious surfaces and $A_{non\text{-}veg}$ is the area of these surfaces. We assumed that $E_{non\text{-}veg}$ is negligibly small compared to ET_{veg} because nonvegetated surfaces are not irrigated and thus have zero or very low evaporation rates. In fact, our chamber measurements consistently indicated nondetectable rates of evaporation when applied to bare soil and

concrete. Also, in a recent study of irrigation impacts on the hydrological cycle of Los Angeles that involved an ensemble of urban canopy models, *Vahmani and Hogue* [2015] showed that without irrigation, industrial/commercial areas had $ET \approx 0$. It should be noted that our ET_{land} estimates do not include the contributions from open water bodies, such as lakes, ponds, and swimming pools.

To investigate the role of social factors in spatial variability of ET_{land}, we plotted ET_{land} of council districts against their MHI (Table 2) [*Thornberg et al*., 2015] and examined whether these variables were correlated.

2.6. Environmental Data

The California Department of Water Resources maintains a California Irrigation Management Information System (CIMIS; cimis.water.ca.gov) that provides ET_0 and other weather parameters from a network of more than 145 weather stations located on irrigated turfgrass lawns, which serve as reference *ET* surfaces. CIMIS ET_0 is calculated using a version of the Penman-Monteith equation (www.cimis.water.ca.gov/content/pdf/PM Equation.pdf) [*Penman*, 1948; *Monteith*, 1965; *Eichinger et al*., 1996; *Pereira and Perrier*, 1999; *Pereira et al*., 2015]. We downloaded monthly averaged ET_0, I_0, temperature, and vapor pressure from the three CIMIS weather stations nearest to Los Angeles (#99—Santa Monica; #133—Glendale; #174—Long Beach; Figure 1) for the years 2007 and 2008, and used temperature and vapor pressure to calculate *D*. We calculated the averages of ET_0, I_0, and *D* for these 2 years, and analyzed their spatial variability. From this analysis, we determined which variables could be averaged and applied to the entire city, and which variables varied spatially and required additional extrapolation for each council district.

2.7. City-Wide *ET* from NLDAS Models

Data sets of monthly *ET* from 1979 to present are available from NLDAS (emc.ncep.noaa.gov/mmb/nldas). We retrieved monthly *ET* from the Noah, Mosaic and VIC models [*Liang et al*., 1994; *Koster and Suarez*, 1996; *Ek*, 2003; *Mitchell et al*., 2004] for Los Angeles and calculated ensemble averages for 2007 and 2008. We did not use *ET* from the SAC model, which does not treat vegetation explicitly [*Mitchell et al*., 2004].

3. Results

3.1. Model Parameters

Among tree species, d_i varied from 0.4 trees ha^{-1} for Aleppo pine (*Pinus halepensis*) and southern magnolia (*Magnolia grandiflora*) to 25 trees ha^{-1} for Italian cypress (*Cupressus sempervirens*, supporting information Table S1). Among council districts, *d* varied from 180 to 418 trees ha^{-1} and k_{mc} varied from 0.61 ± 0.14 to 0.78 ± 0.10 because of the differences in A_{TCC} (Table 2). For the entire city, *d* was 319 trees ha^{-1} and k_{mc} was 0.7 ± 0.12.

Table 2. Land Area (A_{land}), Cumulative Vegetation Cover (A_{veg}), Tree Canopy Cover (A_{TCC}), Area of Low-Density Residential Land Cover (A_{LDR}), Distance from the Coast (*x*), Estimated Number of Trees (N_{Trees}), Tree Density on A_{veg} (*d*), Microclimate Coefficient ($k_{mc} \pm$ Standard Error), Median Household Income (*MHI*), Annual Turfgrass Evapotranspiration (ET_{Grass}), Tree Transpiration (E_{Trees}), Overall Landscape *ET* From Vegetated Area (ET_{veg}), and Overall Landscape *ET* From Land Area (ET_{land}) for Each Los Angeles Council District[a]

Council district	A_{land} (ha)	A_{veg} (ha)	A_{TCC} (ha)	A_{LDR} (ha)	*x* (km)	N_{Trees} ($\times 10^3$)	*d* (trees ha^{-1})	k_{mc}	*MHI* ($)	ET_{Grass} (mm yr^{-1})	E_{Trees} (mm yr^{-1})	ET_{veg} (mm yr^{-1})	ET_{land} (mm yr^{-1})
1	3217	704	512	452	29.2	260.5	370	0.65 ± 0.13	38,674	761 ± 49	361 ± 28	1122 ± 57	246 ± 11
2	8213	2987	2183	5164	24.8	1110.0	372	0.64 ± 0.13	55,024	760 ± 49	360 ± 28	1120 ± 57	407 ± 18
3	9858	3961	2568	7076	19.0	1305.4	330	0.67 ± 0.12	65,860	794 ± 47	317 ± 25	1111 ± 53	446 ± 19
4	6233	2583	1792	2579	21.5	911.2	353	0.66 ± 0.13	58,888	775 ± 48	341 ± 27	1115 ± 55	462 ± 20
5	9841	4794	3661	6918	12.5	1861.3	388	0.63 ± 0.13	64,545	746 ± 50	370 ± 29	1116 ± 58	543 ± 25
6	6899	1764	1032	2721	26.0	524.6	297	0.70 ± 0.12	47,494	820 ± 45	289 ± 23	1109 ± 50	283 ± 12
7	6390	1653	1041	3460	36.4	529.2	320	0.68 ± 0.12	53,662	801 ± 46	315 ± 25	1117 ± 52	289 ± 12
8	4522	1363	482	1922	16.0	245.2	180	0.78 ± 0.10	30,990	915 ± 40	172 ± 14	1087 ± 42	328 ± 12
9	3870	630	291	137	20.5	147.9	235	0.74 ± 0.11	28,883	871 ± 42	226 ± 18	1097 ± 45	179 ± 7
10	3456	741	412	745	16.3	209.4	283	0.71 ± 0.12	36,243	832 ± 44	271 ± 21	1103 ± 49	236 ± 10
11	10,490	4274	2466	4858	3.8	1253.8	293	0.70 ± 0.12	82,596	823 ± 45	275 ± 22	1098 ± 49	447 ± 18
12	11,830	4268	2346	7930	28.6	1192.5	279	0.71 ± 0.11	66,792	834 ± 44	272 ± 21	1107 ± 49	399 ± 16
13	3175	794	434	449	26	220.6	278	0.71 ± 0.11	39,268	836 ± 44	270 ± 21	1106 ± 49	276 ± 11
14	5654	1537	1265	2045	31.2	643.1	418	0.61 ± 0.14	38,032	722 ± 52	409 ± 32	1131 ± 61	308 ± 15
15	8489	1819	757	2167	7.0	384.9	212	0.75 ± 0.11	44,302	889 ± 41	199 ± 16	1089 ± 44	233 ± 9
All city	102,137	33,872	21,243	48,624		10,800	319	0.68 ± 0.12		803 ± 47	307 ± 25	1110 ± 53	368 ± 16

[a]Values of A_{land}, A_{veg}, A_{TCC}, A_{LDR}, N_{Trees}, and *d* are from or based on *McPherson et al*. [2008]; *MHI* is from *Thornberg et al*. [2015]. *ET* values are shown with propagated standard errors; "all city" *ET* values are calculated as weighted sums of the council districts.

There were no significant correlations between A_S measured in urban trees in the Los Angeles region and their *DBH* (Figure 2). However, the ensemble of points had distinct edges that we used to estimate minimum and maximum A_S by the following functions:

$$A_{Smax} = 91.64 - 9.47 \times DBH + 1.08 \times DBH^2 - 0.01 \times DBH^3 \quad (11a)$$

for the upper limit and

$$A_{Smin} = -132.75 + 11.34 \times DBH \text{ for the lower limit of } A_S. \quad (11b)$$

For A_{Smax}, $R^2 = 0.98$ and for A_{Smin}, $R^2 = 0.91$ ($p < 0.0001$ for both). Using equations (11), we estimated A_{Smax} and A_{Smin} of Los Angeles trees by substituting *DBH* from the survey by *Nowak et al.* [2010] and calculated mean A_S for each species by averaging these two extremes. The resulting A_S estimates were up to 1990 ± 1100 cm^2 for flowering trees and up to 1700 ± 950 cm^2 for coniferous trees; 50% of flowering trees and 80% of coniferous trees had $A_S < 200$ cm^2 (Figure 3; supporting information Table S1).

3.2. Weather Parameters

ET_0 and I_0 had similar seasonal patterns without systematic differences among CIMIS weather stations (Figure 4). To approximate ET_0 and I_0 in the city of Los Angeles, we calculated ensemble averages of weather data. The resulting ET_0 varied from 1.5 ± 0.2 mm d^{-1} in December to 4.8 ± 0.2 mm d^{-1} in June. I_0 varied from 98 ± 11 W m^{-2} in December to 288 ± 10 W m^{-2} in June (Figure 4).

D varied from a minimum of 0.17 ± 0.01 kPa in May (CIMIS weather station "Long Beach") to a maximum of 1.09 ± 0.17 kPa in October (CIMIS weather station "Glendale"). Unlike ET_0 and I_0, *D* did not exhibit a clear seasonal pattern, yet had a pronounced coast-to-inland gradient during summer (Figure 4). Therefore, to approximate *D* in the city of Los Angeles, we considered the relationships between *D* and distance from the coast (x). To increase the sample size of *D*, we also used data from two additional CIMIS weather stations near Los Angeles (#78—Pomona; #159—Monrovia). There was a significant linear correlation between *x* and *D* for the months of June through September. Thus, we developed linear functions (Figure 5) to approximate *D* in each council district from the distance of its centroid to the coast (Table 2). For the rest of the year, *D* and *x* were not correlated, and we approximated *D* in Los Angeles as an ensemble average, similar to ET_0 and I_0 (Figure 4).

3.3. Annual Landscape *ET*: Council Districts

ET_{veg} varied from 1087 ± 42 to 1131 ± 61 mm yr^{-1}, due to variability in ET_{Grass} and E_{Trees} among the districts (Table 2; Figure 6). Maps of ET_{Grass} and E_{Trees} are shown on supporting information Figures S1–S4. ET_{land} varied from 179 ± 7 to 543 ± 25 mm yr^{-1}, due to differences in ET_{veg} and vegetation cover of each district (Table 2; Figure 6). Total ET_{veg} and ET_{land} of Los Angeles, calculated as the weighted sum of all districts, equaled 1110 ± 53 and 368 ± 16 mm yr^{-1}, respectively (Table 2).

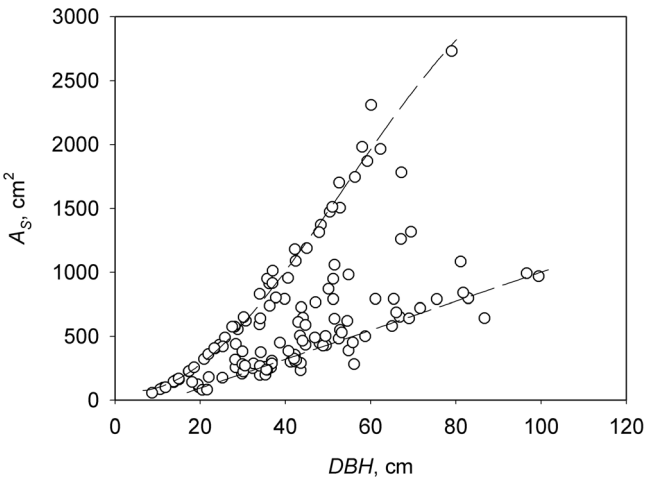

Figure 2. Measured sapwood areas (A_S) of 115 trees in the Los Angeles metropolitan area versus diameter at breast height (*DBH*). The ensemble of points has distinct upper and lower limits that we approximated by the equations (11a) and (11b) in the text.

ET_{land} was linearly correlated with *MHI* (Table 2) [*Thornberg et al.*, 2015] across the council districts (Figure 7; $R^2 = 0.62$; $p = 0.0003$).

3.4. Monthly Landscape *ET*: The City of Los Angeles

ET_{Grass} from the cumulative vegetated area of Los Angeles varied from 1.1 ± 0.1 to 3.3 ± 0.2 mm d^{-1}, and E_{Trees} varied from 0.4 ± 0.0 to 1.1 ± 0.1 mm d^{-1}, reaching minima in December and maxima in June (Figure 8). Flowering trees (71% of all trees) were responsible for 94% of total tree transpiration during the growing season and 91% during winter. Coniferous trees were responsible for 5% during

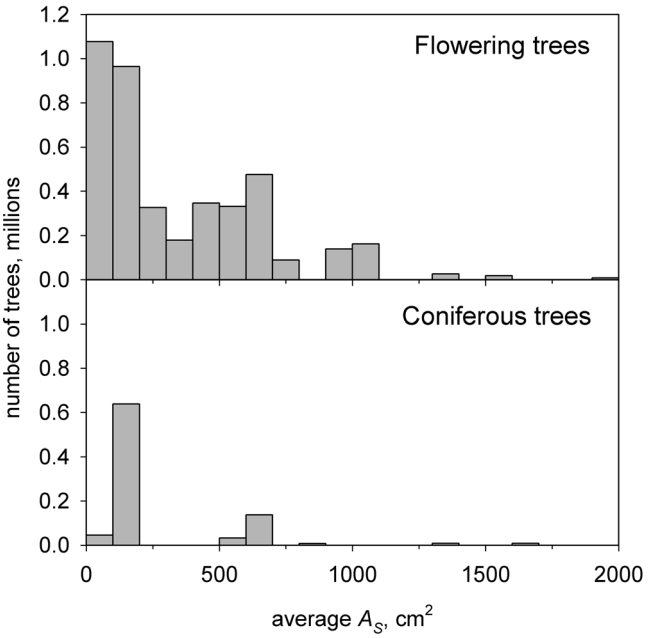

Figure 3. Distribution of modeled A_S of Los Angeles trees.

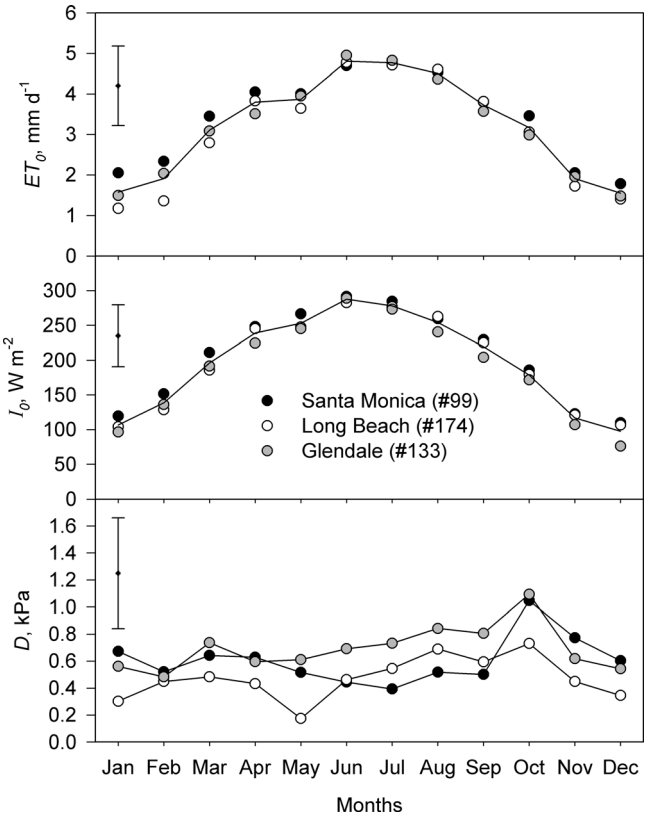

Figure 4. Monthly averaged reference evapotranspiration (ET_0), incoming solar radiation (I_0), and vapor pressure deficit of the air (D) from California Irrigation Management Information System (CIMIS) weather stations nearest to Los Angeles. Error bars show one average standard deviation of daily values from their monthly means.

the growing season and 7% during winter, and palms were responsible for 1% year round.

ET_{veg} varied from 1.5 ± 0.1 mm d^{-1} in December to 4.3 ± 0.2 mm d^{-1} in June (Figure 8). On average, turfgrass and trees contributed 70% and 30% to total ET, respectively. ET_{land} was three times smaller than ET_{veg}, which reflects the fractional cover of vegetation on the total land area of the city (equation (10)); ET_{land} varied from 0.48 ± 0.02 mm d^{-1} in December to 1.4 ± 0.1 mm d^{-1} in June (Figure 8). ET_{veg} was very close to ET_0 from CIMIS stations near Los Angeles, never deviating by more than 10% (Figures 8 and 9).

ET from NLDAS varied from 0.12 ± 0.08 mm d^{-1} in January to 1.4 ± 0.3 mm d^{-1} in June, on total land area. ET from NLDAS was similar to our estimates in May and June, but smaller in all other months (Figures 8 and 9).

4. Discussion

We estimated ET in Los Angeles using empirical models based on in situ measurements of turfgrass ET and tree transpiration and previously developed spatial maps of land cover. To the best of our knowledge, these are the first estimates of municipal scale ET that discern relative contributions from different growth forms (turfgrass and trees) and tree species (Figure 8 and supporting information Figures S1–S4). ET from vegetated areas only was 1110 ± 53 mm yr^{-1} and ET from total land area of Los Angeles (including nonvegetated surfaces) was 368 ± 16 mm yr^{-1}. Turfgrass contributed ~70% to total landscape ET, and trees (the majority of which were flowering) contributed the remaining ~30%.

Monthly ET_{veg} was very close to CIMIS ET_0, which represents ET of unshaded irrigated turfgrass that has access to nonlimited soil water and closely corresponds to maximum ET of well-watered vegetated surfaces (Figures 8 and 9). Los Angeles landscapes in this study were indeed well-watered,

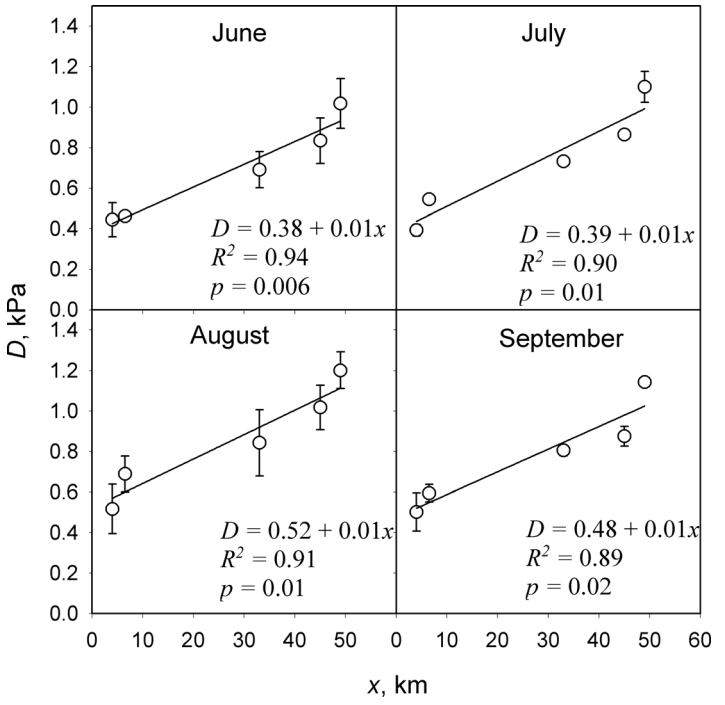

Figure 5. Monthly averaged vapor pressure deficit of the air (*D*) at CIMIS weather stations versus their distances from the coast (*x*): #99—Santa Monica, 4.0 km; #174—Long Beach, 6.5 km; #133—Glendale, 33 km; #78—Pomona, 45 km; #159—Monrovia, 49 km. Error bars show one standard error.

as in situ measurements underlying the models of *ET* (equations (3), (4), and (6)) detected no significant impacts of temporal variations in soil water on *ET* of studied trees and turfgrass [*Litvak and Pataki*, 2016; *Litvak et al.*, 2017]. In addition, the landscapes were comprised of two canopy layers (trees and turfgrass), and subjected to an "oasis effect," i.e., advective enhancement of *ET* from relatively dense vegetation surrounded by hotter, nonvegetated urban areas [*Oke*, 1979; *Potchter et al.*, 2008; *Chang and Li*, 2014; *Chow et al.*, 2014; *Rahman et al.*, 2017; *Zipper et al.*, 2017]. For example, in the study in Minneapolis—Saint Paul, Minnesota, *Peters et al.* [2011] observed that annual *ET* from recreational areas covered with trees and turfgrass was ~44% higher than *ET* from residential areas, with the error of water flux measurements within 20%.

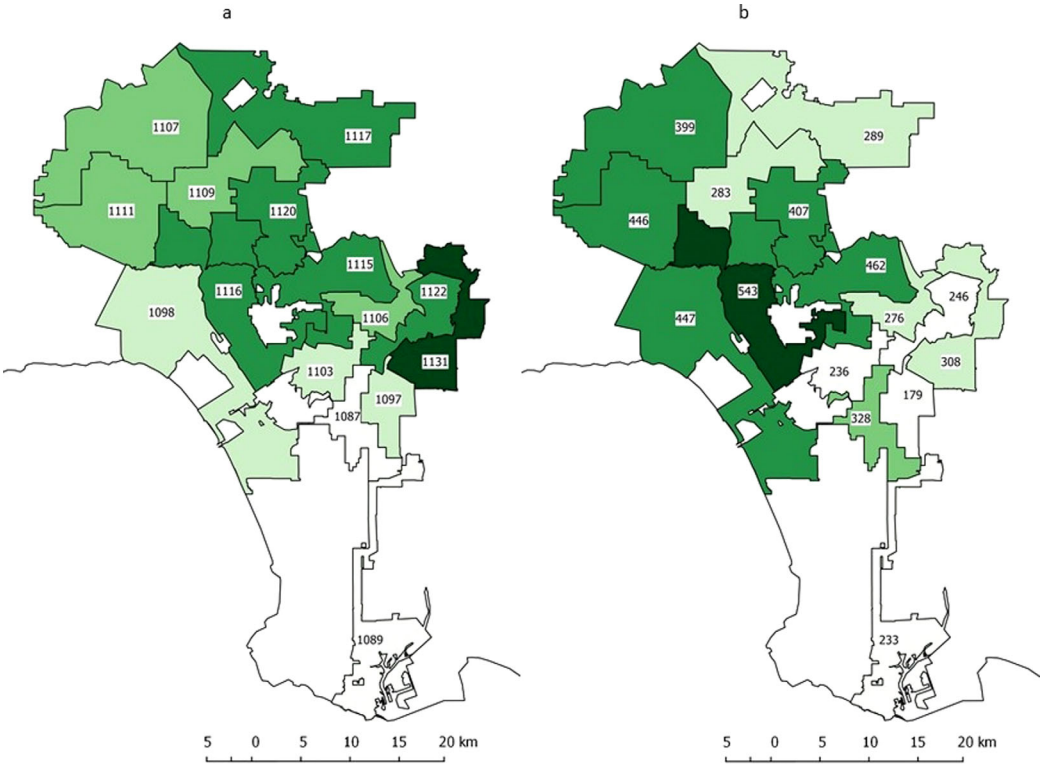

Figure 6. Modeled annual *ET* (mm yr^{-1}) from (a) cumulative vegetated areas (ET_{veg}) and (b) total land areas (ET_{land}) estimated for Los Angeles council districts (Table 2).

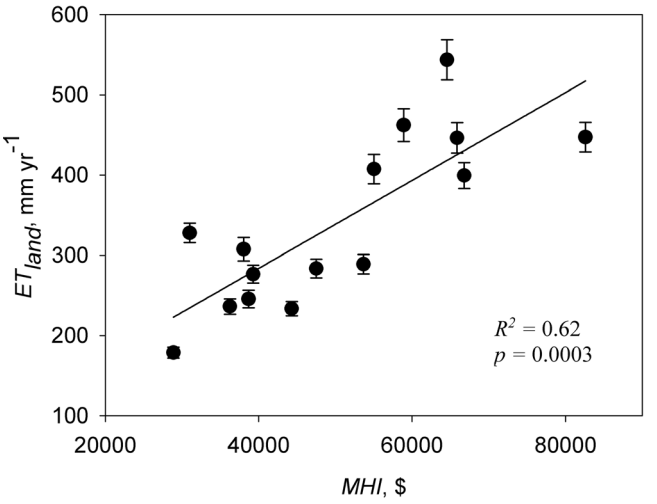

Figure 7. Modeled annual *ET* from total land areas of Los Angeles council districts (ETland, mm yr^{-1}) versus median household income (*MHI*, $; Table 2) [*Thornberg et al.*, 2015]. Error bars show 1 propagated standard error of the linear regression.

Therefore, similarity between ET_{veg} of a well-watered Los Angeles landscapes and CIMIS ET_0 is reasonable. Even though E_{Trees} was significantly smaller than ET_0, ET_{Grass}, and even the reduction of summertime ET_{Grass} caused by shading from tree canopies [*Litvak et al.*, 2014], this shading was not sufficient to offset *ET* from the vast expanse of irrigated turfgrass that provided the bulk of ET_{veg} (Figure 8).

Yearly ET_{veg} was also similar to *ET* of dense meadows in the Owens Valley of California at the base of the Sierra Nevada Mountain range, which have the highest *ET* among native landscapes in California [*Duell*, 1991; *Steinwand et al.*, 2006]. In addition, yearly ET_{veg} was similar to an irrigated park in a dry Mediterranean region of Adelaide, Australia [*Nouri et al.*, 2016]. It was also within the range of transpiration from tropical tree plantations (1000–1500 mm d^{-1}) [*Larcher*, 2001].

4.1. Performance of NLDAS Models

Yearly *ET* was 1.6 times larger than NLDAS model predictions, but peak *ET* values in May and June agreed with NLDAS (Figure 8). While the overall magnitude and general annual patterns of *ET* are relatively similar to our empirically based *ET*, the NLDAS models largely underestimated *ET* most of the time (Figures 8 and 9).

NLDAS *ET* has estimated errors <5 mm/month [*Long et al.*, 2014]. However, NLDAS was not designed to represent the complex composition of the Los Angeles landscape and variable responses of irrigated plants to urban microclimates. NLDAS models used in this study (Noah, Mosaic, and VIC) compute *ET* as a fraction of potential *ET* derived with Penman-Monteith equation [*Mahrt and Ek*, 1984], using parameters that represent (1) soil moisture, (2) fractional vegetation cover, and (3) surface resistance [Noah—*Chen et al.*, 1996; Mosaic—*Koster and Suarez*, 1994;

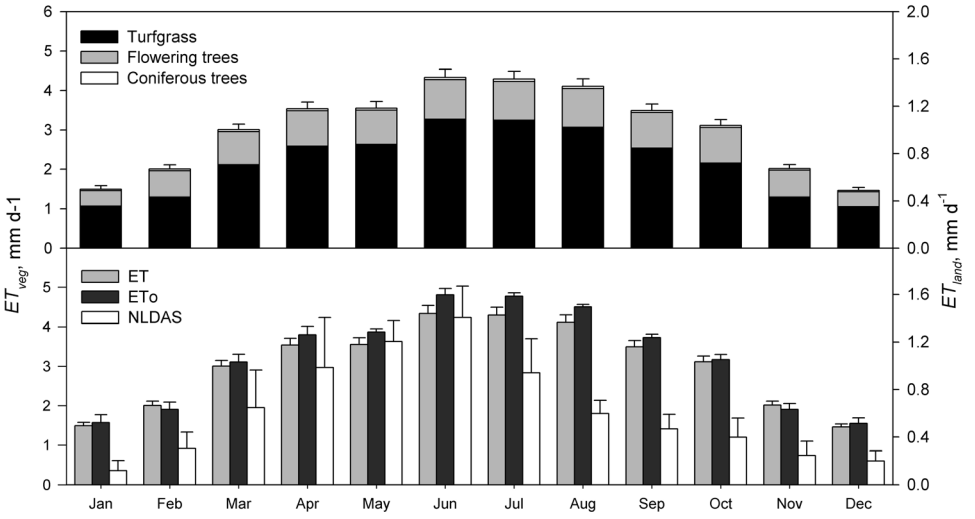

Figure 8. Modeled *ET* from cumulative vegetated areas in Los Angeles (ET_{veg}, left axis) and from the total land area of the city (ET_{land}, right axis). (top) *ET* obtained from our empirical models based on in situ measurements with contributions from turfgrass, flowering trees, and coniferous trees. (bottom) *ET* obtained from our empirical models based on in situ measurements (same as top), with average ET_0 from CIMIS weather stations and the ensemble of land surface models within the NLDAS framework. Error bars show 1 propagated standard error of the linear regression.

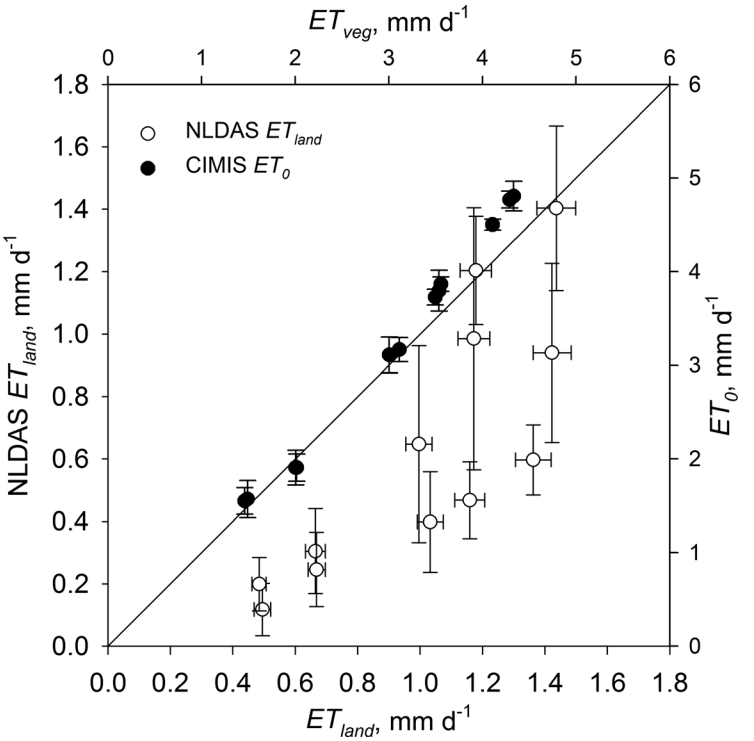

Figure 9. Average monthly *ET* from the ensemble of land surface models within the NLDAS framework (NLDAS ET_{land}, left axis) plotted against our empirically based monthly ET from the total land area of the city (ET_{land}, bottom axis) and average monthly ET_0 from CIMIS weather stations (right axis) plotted against our empirically based monthly *ET* from cumulative vegetated areas in Los Angeles (ET_{veg}, top axis), shown with 1:1 line. Error bars show 1 propagated standard error of the linear regression.

VIC—*Liang et al.*, 1994]. The associated errors are (1) underestimation of soil moisture caused by the absence of irrigation module, (2) misrepresentation of urban canopy because model grids (~14 km) are larger than the scale of urban heterogeneity [*Monaghan et al.*, 2014], and (3) inaccurate representation of urban canopy resistance that deviates from Penman-Monteith scheme [*Litvak et al.*, 2017].

Incorporation of an irrigation module into Noah LSM coupled with an urban canopy model significantly improved representation of *ET* in the Los Angeles metropolitan area that was otherwise largely underestimated [*Vahmani and Hogue*, 2014a,b,]. Similarly, in the study in Houston, Texas, the inclusion of an irrigation module and adding fractional urban canopy cover within each grid to the model input resulted in increased accuracy of land surface temperatures that were otherwise largely overestimated [*Monaghan et al.*, 2014]. Despite the simplicity of the irrigation scheme used by *Monaghan et al.* [2014]—it simulated permanent uninterrupted irrigation of all greater Houston—it led to more realistic representation of latent heat flux compared to the original models. Unfortunately, direct comparison of our estimates with ET produced by such high resolution models was impractical because in their current state these models may not be applied to large heterogeneous areas such as Los Angeles municipal districts.

Also, model performance may be improved for areas of interest by means of calibration, but this is a challenging task because of the complexity of the models [*Friedl*, 1996]. In fact, from the models considered here, only Noah was calibrated using ground-based latent heat fluxes, yet the ground data did not cover Los Angeles [*Wei et al.*, 2013], while Mosaic and VIC were not calibrated to match *ET* [*Mitchell et al.*, 2004; *Troy et al.*, 2008].

In summary, more accurate predictions of *ET* in Los Angeles may be achieved by adding an irrigation module, improving representation of subgrid spatial vegetation coverage, and calibrating the models using ground-based assessments of *ET*.

4.2. Sources of Uncertainty in our Empirical *ET* Estimates

Overall, we obtained *ET* estimates using the same equations for the entire city. These estimates do not take into account variations in species composition, stand age, soil compaction, micrometeorological conditions, and irrigation and management practices across the city. We used the empirical models derived from the measurements of mature healthy trees and well-maintained turfgrass lawns. One may expect a substantial difference between ET of such model landscapes and real-life landscapes that consist of an uncertain combination of young and mature, healthy and damaged plants. However, at the current state of knowledge, we could not predict the effects of such factors on municipal scale *ET*.

Uncertainty of ET_{veg} was dominated by uncertainty of ET_{Grass}, which appeared to be the largest contributor to landscape ET (Figure 8). ET_{Grass} was highly influenced by shading that we estimated using fractional tree cover over turfgrass, A_{TCC}/A_{veg} (equation (4)). In fact, ET_{Grass} was not very sensitive to small deviations of A_{TCC} (a 5–15% change of A_{TCC} caused a 4–7% change in ET_{Grass}). In addition, we assumed after *McPherson et al.* [2008] that turfgrass occupied all space under tree canopies. This is clearly an upper limit, and the actual turfgrass cover under trees may be somewhat lower. According to *Litvak and Pataki* [2016], every 10% reduction of turfgrass cover under trees may lead to an approximately 5% reduction in ET_{Grass}. Therefore, even with greater shading and lower turfgrass cover under trees, ET_{Grass} would still dominate ET_{veg}.

However, in actual urban landscapes, shading is not only provided by tree canopies, but also by buildings and other structures, and varies by extent, intensity, and temporal (diurnal and seasonal) patterns. According to in situ measurements, there is >10-fold variability in plot-scale ET_{Grass} of Los Angeles lawns caused by a diversity of shading regimes and environmental conditions [from 10% to over 110% of CIMIS ET_0; *Litvak and Pataki*, 2016]. Taking this variability into account would greatly improve precision and spatial representation of ET_{Grass}. This may be achieved by integrating ground-based assessments of ET_{Grass} into spatially resolved numeric models capable of more detailed representation of shading or integration with high resolution remote sensing information. Nevertheless, the linear scaling used in this study provides robust first-order estimates of ET_{Grass} because of its strong linear relationship with I_0 established in previous studies [*Feldhake et al.*, 1983; *Abtew and Melesse*, 2013; *Litvak et al.*, 2014].

Another major source of uncertainty is the landscape composition. Because of tremendous species variability and spatial heterogeneity, surveying plant diversity and species composition in Los Angeles is challenging [*Nowak et al.*, 2010; *Avolio et al.*, 2015; *Jenerette et al.*, 2016]. Thus, municipal-scale surveys of shrub and nonturf groundcover species composition do not currently exist for Los Angeles. The survey of plant canopy cover we used in this study does not distinguish shrubs from trees and turfgrass from other irrigated groundcovers [*McPherson et al.*, 2008]. As a consequence, we modeled transpiration of all ornamental plants as either E_{Trees} or ET_{Grass}, which introduces uncertainty in actual transpiration patterns. In addition, ET_{veg} is subject to inevitable scaling errors that stem from using in situ measurements of subset of species at specific locations to model E_{Trees} and ET_{Grass} [*Litvak and Pataki*, 2016; *Litvak et al.*, 2017].

4.3. Spatial Variability of *ET*

ET_{veg} was relatively uniform among council districts (~1100 mm yr^{-1}; Figure 6a; Table 2), with ET_{Grass} responsible for 64–84% of the total. The difference between maximum ET_{veg} (council district 14) and minimum ET_{veg} (council district 8) was 44 mm yr^{-1}, which is within the limits of the standard error (Table 2).

In contrast to ET_{veg}, there was a threefold difference in ET_{land} among council districts (179–543 mm yr^{-1}; Figure 6b; Table 2) caused by differences in fractional vegetation cover. Previous studies showed that higher vegetation cover in afforested cities may be associated with more affluent neighborhoods that are comprised of larger parcels and may invest more in landscape management ("luxury effect") [*Clarke et al.*, 2013; *Huang et al.*, 2011; *Jenerette et al.*, 2007]. In Los Angeles, the luxury effect leads to cooler microclimates in affluent neighborhoods and was shown to cause a decrease in average land surface temperatures of 0.05–0.75°C for each increase in neighborhood income of $10,000 [*Clarke et al.*, 2013].

Our results support these findings. ET_{land} was linearly correlated with *MHI* across the council districts (Figure 7; $R^2 = 0.62$; $p = 0.0003$). Moreover, *MHI* was linearly correlated with the area of low-density residential development (A_{LDR}; Table 2; $R^2 = 0.50$; $p = 0.0019$), as well as fractional vegetation cover (A_{veg}/A_{land}; $R^2 = 0.63$; $p = 0.0003$) and fractional tree canopy cover (A_{TCC}/A_{land}; $R^2 = 0.45$; $p = 0.004$) across the council districts (linear regressions not shown). This supports suggestions that more affluent council districts have higher fractional cover of turfgrass and trees resulting in larger ET_{land} that potentially leads to cooler microclimates due to the combination of shading from tree canopies and evaporative cooling.

In addition, coastal areas of the Los Angeles basin are characterized by a more humid climate than inland areas, and temperature and aridity increase with distance from the coast [*Clarke et al.*, 2013; *Tayyebi and Jenerette*, 2016]. This coast-to-inland climate gradient determines the natural distribution of plants in non-urbanized areas and may also play a role in the spatial distribution of urban vegetation. On one hand, climatic conditions are more favorable for plant growth in coastal areas. On the other hand, there is a greater need for shady trees in hotter and drier inland portion of the city [*Clarke et al.*, 2013; *Tayyebi and Jenerette*,

2016]. While no relationship has been found between A_{TCC} and distance from the coast [*Clarke et al*., 2013], ground surveys have confirmed that large shade trees are more prevalent in the inland areas [*Avolio et al*., 2015]. Our analysis did not reveal an influence of the coast-to-inland climate gradient on spatial variations of ET_{veg} and ET_{land}. Likely, this reflects the ecological similarity of irrigated urban yards, which is a result of a relatively uniform urban development that reduces microclimate variation [*Groffman et al*., 2014; *Hall et al*., 2016].

4.4. Implications for Water and Landscape Management

Regional effects of climate change are giving rise to a significant reduction of water supply in California that poses acute challenges for highly populated urban regions [*Barnett et al*., 2008; *Hanak and Lund*, 2008; *Melillo et al*., 2014]. Since 2007, California has been affected by unprecedented drought conditions [*MacDonald*, 2010; *Aghakouchak*, 2015; *Diffenbaugh et al*., 2015]. In 2009, mandatory water conservation measures were launched, and in 2014, "emergency restrictions" were implemented [*California Department of Water Resources*, 2009; *LADWP*, 2016b]. Prior to these measures, more than 50% of household water in Los Angeles was used outdoors [*DeOreo et al*., 2011; *Mini et al*., 2014]. At the same time, 86% of Los Angeles municipal water is delivered from remote locations via a large-scale system of aqueducts [*Cohen et al*., 2004, *Hanak et al*., 2011, *Hughes et al*., 2013, *LADWP*, 2016a, *Sanders*, 2016], with nearly 100 agencies involved in managing water supply and distribution [*Pincetl et al*., 2016].

Sustaining irrigated urban landscapes under restricted water availability and complex water supply systems calls for a robust quantitative understanding of water use by urban vegetation [*Hogue and Pincetl*, 2015]. The assessment of Los Angeles *ET* presented in this study has direct implications for developing effective water-saving measures and minimizing undesirable trade-offs.

Our results suggest that turfgrass dominates *ET* in Los Angeles and could be targeted for water conservation measures. Without trees, unshaded turfgrass would lead to ET_{veg} of 1060–1300 mm yr^{-1} across Los Angeles (assuming $0.9 \leq k_{mc} \leq 1.1$) [*Litvak and Pataki*, 2016]. In a previous study, we reported excessive irrigation practices in the Los Angeles region compared to municipal watering recommendations [*Costello et al*., 2000; *Litvak and Pataki*, 2016]. Unshaded lawns that had the highest *ET* received at least 40% more irrigation than municipal recommendations according to in situ *ET* measurements in summer 2010 [*Litvak and Pataki*, 2016]. In addition, municipal guidelines tend to overestimate actual turfgrass *ET* [*Litvak and Pataki*, 2016]. Current recommendations do not adequately recognize seasonal changes of urban microclimatic conditions that lead to higher than necessary watering recommendations in winter [*Litvak and Pataki*, 2016].

Irrigated landscapes alleviate urban heat and reduce the need for air conditioning [*Akbari*, 2002; *Jenerette et al*., 2007; *Thom et al*., 2016; *Wang et al*., 2016b]. Therefore, restricting irrigation is sometimes considered as a trade-off between water and energy savings [*Yang and Wang*, 2015]. However, while turfgrass is the largest component of *ET*, urban trees can reduce the energy costs of air conditioning by up to 50% [*Akbari*, 2002; *Simpson*, 2002; *Jenerette et al*., 2011]. In addition, shade from urban trees improves human thermal comfort by providing immediate local cooling [*Shashua-Bar et al*., 2009, 2011; *Rahman and Ennos*, 2016]. On the other hand, evaporative cooling from well-irrigated turfgrass may have significant impacts at municipal and regional scales, reducing mean air temperatures and alleviating the urban heat island effect [*Rahman and Ennos*, 2016]. Therefore, it is important to distinguish between spatial scales of cooling caused by *ET* and by shade that reduces solar radiation reaching streets and buildings. Evaporative cooling is provided by both turfgrass and trees, with the largest effects from nonwater-limited turfgrass, while shading of buildings and streets is provided by tree canopies only [*Rahman and Ennos*, 2016]. While cooling effects from tree shade are relatively well understood and quantified [*Akbari*, 2002; *Simpson*, 2002; *Jenerette et al*., 2007; *Clarke et al*., 2013; *Litvak et al*., 2014; *Thom et al*., 2016; *Wang et al*., 2016b], regional evaporative cooling is more difficult to address as it depends on the atmospheric dynamics of the city and its surroundings. Therefore, quantifying regional cooling requires advanced models that are well developed and parameterized for urban conditions [*Yang and Wang*, 2015], including accurate estimates of *ET*. Nevertheless, despite the importance and complexity of the trade-off between water and every savings, cities in dry environments continue to experience restricted water supplies and reducing irrigation will likely be a necessity. Estimates of urban plant *ET* resolved by plant type can contribute to optimizing the tradeoffs between reducing irrigation and altering surface energy balance.

5. Conclusions

In the dry southwestern U.S., large proportions of municipal water budgets are used for landscape irrigation/outdoor water use [*St. Hilaire et al*., 2008; *Sabo et al*., 2010; *Melillo et al*., 2014; *Mini et al*., 2014]. Accurate estimates of municipal scale *ET* from irrigated urban landscapes are critically important for cities located in naturally dry environments, where water conservation is a priority [*Sabo et al*., 2010; *Pataki et al*., 2011a; *Chow et al*., 2014]. In this study, we estimated *ET* of irrigated landscapes in Los Angeles upscaled from in situ measurements of plot-scale turfgrass *ET* and tree transpiration (Figure 6). ET_{veg} was close to ET_0 (Figures 8 and 9), suggesting that water availability of vegetation was not limited because of adequate or excess irrigation. Irrigated turfgrass was responsible for 64–84% of total ET_{veg} depending on differences in vegetation cover among council districts. ET_{land} linearly increased with *MHI* across districts that corresponded to higher vegetation cover and possibly enhanced human thermal comfort in more affluent districts (Figure 7). NLDAS models underestimated ET_{land} most part of the year, which we attributed to the lack of irrigation modules in these models and a model resolution/urban heterogeneity scale mismatch. Our results highlight the large flux of *ET* in this semiarid region caused by urbanization and associated changes in vegetation cover, plant functional type, and irrigation.

Acknowledgments

We thank Ray Anderson for a valuable advice and anonymous reviewers for their insightful comments that greatly improved this article. This research was supported by the National Science Foundation grants EAR 1204442 and IOS 1147057. The original data set used in this study was collected on the properties of UC Irvine, the City of Los Angeles, the Los Angeles Zoo and Botanical Gardens, the Los Angeles County Arboretum and Botanic Garden, the Los Angeles Police Academy, and Fullerton Arboretum, with valuable assistance by Stephanie Pincetl, Neeta Bijoor, Thomas Gocke, Christine Goedhart, Michael Kazzi, Ilya Litvak, Eric Nguyen, Sonja Djuricin, and Amy Townsend-Small. The data used are listed in the references, tables, and supplements.

References

Abtew, W., and A. Melesse (2013), *Evaporation and Evapotranspiration—Measurements and Estimations*, Springer, Dordrecht, Heidelberg, New York, London.

Aghakouchak, A. (2015), Recognize anthropogenic drought, *Nature*, *524*, 409–411.

Akbari, H. (2002), Shade trees reduce building energy use and CO_2 emissions from power plants, *Environ. Pollut.*, *116*(Suppl. 1), 119–126, doi:10.1016/S0269-7491(01)00264-0.

Aminzadeh, M., and D. Or (2017), The complementary relationship between actual and potential evaporation for spatially heterogeneous surfaces, *Water Resour. Res.*, *53*, 580–601, doi:10.1002/2016WR019759.

Anderson, C. A., and E. R. Vivoni (2016), Impact of land surface states within the flux footprint on daytime land-atmosphere coupling in two semiarid ecosystems of the Southwestern U.S., *Water Resour. Res.*, *52*, 4785–4800, doi:10.1002/2015WR018016.

Avolio, M. L., D. E. Pataki, T. W. Gillespie, G. D. Jenerette, H. R. McCarthy, S. Pincetl, and L. Weller Clarke (2015), Tree diversity in southern California's urban forest: The interacting roles of social and environmental variables, *Frontiers Ecol. Evol.*, *3*(July), 1–15, doi:10.3389/fevo.2015.00073.

Balogun, A., J. Adegoke, S. Vezhapparambu, M. Mauder, J. McFadden, and K. Gallo (2009), Surface energy balance measurements above an exurban residential neighbourhood of Kansas City, Missouri, *Boundary Layer Meteorol.*, *133*(3), 299–321, doi:10.1007/s10546-009-9421-3.

Barnett, T. P., et al. (2008), Human-induced changes in the hydrology of the Western United States, *Science*, *319*, 1080–1083.

Bijoor, N. S., D. E. Pataki, D. Haver, and J. S. Famiglietti (2014), A comparative study of the water budgets of lawns under three management scenarios, *Urban Ecosyst.*, *17*(4), 1095–1117, doi:10.1007/s11252-014-0361-4.

Boegh, E., et al. (2009), Remote sensing based evapotranspiration and runoff modeling of agricultural, forest and urban flux sites in Denmark: From field to macro-scale, *J. Hydrol.*, *377*(3–4), 300–316, doi:10.1016/j.jhydrol.2009.08.029.

California Department of Water Resources (2009), *Water Conservation Act of 2009—The Law*, California Senate, Senate Bill No. 7. [Available at http://www.water.ca.gov/wateruseefficiency/sb7/docs/SB7-7-TheLaw.pdf.]

Carrow, R. N., R. C. Sherman, and J. R. Watson (1990), Turfgrass, in *Irrigation of Agricultural Crops*, edited by B. A. Stewart and D. R. Nielsen, pp. 889–919, Am. Soc. of Agronomy, Inc. Madison, Wis.

Chang, C.-R., and M.-H. Li (2014), Effects of urban parks on the local urban thermal environment, *Urban For. Urban Green.*, *13*, 672–681, doi:10.1016/j.ufug.2014.08.001.

Chen, F., K. Mitchell, J. Schaake, Y. Xue, H.-L. Pan, V. Koren, Q. Y. Duan, M. Ek, and A. Betts (1996), Modeling of land surface evaporation by four schemes and comparison with FIFE observations, *J. Geophys. Res.*, *101*(D3), 7251, doi:10.1029/95JD02165.

Chow, W. T. L., T. J. Volo, E. R. Vivoni, G. D. Jenerette, and B. L. Ruddell (2014), Seasonal dynamics of a suburban energy balance in Phoenix, Arizona, *Int. J. Climatol.*, *34*(15), 3863–3880, doi:10.1002/joc.3947.

Clarke, L. W., G. D. Jenerette, and A. Davila (2013), The luxury of vegetation and the legacy of tree biodiversity in Los Angeles, CA, *Landscape Urban Plann.*, *116*(May), 48–59, doi:10.1016/j.landurbplan.2013.04.006.

Cohen, R., G. Wolff, and B. Nelson (2004), *Energy Down the Drain. The Hidden Costs of California Water Supply*, Natl. Resour. Def. Counc., Pac. Inst., Oakland, Calif.

Costello, L. R., N. Matheny, J. Clark, and K. Jones (2000), *A Guide to Estimating Irrigation Water Needs of Landscape Plantings in California. The Landscape Coefficient Method and WUCOLS III*, Univ. of Calif. Coop. Ext., Calif. Dep. of Water Resour., Sacramento, Calif.

DeOreo, W. B., et al. (2011), *California Single-Family Water Use Efficiency Study*, Aquacraft, Inc. Water Engeneering and Management, Boulder, Colo.

de Vries, J. J., and I. Simmers (2002), Groundwater recharge: An overview of process and challenges, *Hydrogeol. J.*, *10*(1), 5–17, doi:10.1007/s10040-001-0171-7.

Diffenbaugh, N. S., D. L. Swain, and D. Touma (2015), Anthropogenic warming has increased drought risk in California, *Proc. Natl. Acad. Sci. U. S. A.*, *112*(13), 3931–3936, doi:10.1073/pnas.1422385112.

Duell, L. F. W. J. (1991), Estimates of evapotranspiration in alkaline scrub and meadow communities of Owens Valley, California, using the Bowen-ratio, eddy-correlation and Penman-combination methods, in *Geology and Water Resources of Owens Valley, California. Water-Supply Paper 2370-B*, pp. E1–E33, U.S. Geol. Surv., in cooperation with Inyo County and the Los Angeles Department of Water and Power, Washington, D. C.

Dwyer, J. F., D. J. Nowak, M. H. Noble, and S. M. Sisinni (2000), Connecting people with ecosystems in the 21st century: An assessment of our nation's urban forests, *A Technical Document Supporting the 2000 USDA Forest Service RPA Assessment*, U.S. Dep. of Agric., For. Serv., Evanston, Ill.

Eichinger, W. E., M. B. Parlange, and H. Stricker (1996), On the concept of equilibrium evaporation and the value of the Priestley-Taylor coefficient, *Water Resour. Res.*, *32*(1), 161, doi:10.1029/95WR02920.
Ek, M. B. (2003), Implementation of Noah land surface model advances in the National Centers for Environmental Prediction operational mesoscale Eta model, *J. Geophys. Res.*, *108*(D22), 8851, doi:10.1029/2002JD003296.
Feldhake, C., R. Danielson, and J. Butler (1983), Turfgrass evapotranspiration. I. Factors influencing rate in urban environments, *Agron. J.*, *75*(October), 824–830.
Friedl, M. A. (1996), Relationships among remotely sensed data, surface energy balance, and area-averaged fluxes over partially vegetated land surfaces, *J. Appl. Meteorol.*, *35*(11), 2091–2103, doi:10.1175/1520-0450(1996)035<2091:Rarsds>2.0.Co;2.
Goulden, M. L., R. G. Anderson, R. C. Bales, A. E. Kelly, M. Meadows, and G. C. Winston (2012), Evapotranspiration along an elevation gradient in California's Sierra Nevada, *J. Geophys. Res.*, *117*, G03028, doi:10.1029/2012JG002027.
Grimmond, C. S. B., and T. R. Oke (1999), Evapotranspiration rates in urban areas, in *Impacts of Urban Growth on Surface Water and Groundwater Quality, Proceedings of IUGG 99 Symposium HS5, Birmingham, IAHS Publ. 259*, pp. 235–243, IAHS Publ., Wallingford, Oxfordshire, U. K.
Grimmond, C. S. B., C. Souch, and M. D. Hubble (1996), Influence of tree cover on summer-time surface energy balance fluxes, San Gabriel Valley, Los Angeles, *Clim. Res.*, *6*, 45–57.
Groffman, P. M., et al. (2014), Ecological homogenization of urban USA, *Frontiers Ecol. Environ.*, *12*(1), 74–81, doi:10.1890/120374.
Hall, S. J., et al. (2016), Convergence of microclimate in residential landscapes across diverse cities in the United States, *Landscape Ecol.*, *31*, 101–117, doi:10.1007/s10980-015-0297-y.
Hamlet, A. F., P. W. Mote, M. P. Clark, and D. P. Lettenmaier (2007), Twentieth-century trends in runoff, evapotranspiration, and soil moisture in the western United States, *J. Clim.*, *20*(8), 1468–1486, doi:10.1175/JCLI4051.1.
Hanak, E., and J. Lund (2008), *Adapting California's Water Management to Climate Change*, San Francisco, Calif.
Hanak, E., J. Lund, A. Dinar, B. Gray, R. Howitt, J. Mount, P. Moyle, and B. "Buzz" Thompson (2011), *Managing California's Water From Conflict to Reconciliation*, Publ. Policy Inst. of Calif., San Francisco, Calif.
Hart, Q. J., M. Brugnach, B. Temesgen, C. Rueda, S. L. Ustin, and K. Frame (2009), Daily reference evapotranspiration for California using satellite imagery and weather station measurement interpolation, *Civ. Eng. Environ. Syst.*, *26*(1), 19–33, doi:10.1080/10286600802003500.
Hogue, T. S., and S. Pincetl (2015), Are you watering your lawn?, *Science*, *348*(6241), 1319–1320, doi:10.1126/science.aaa6909.
Huang, G., W. Zhou, and M. L. Cadenasso (2011), Is everyone hot in the city? Spatial pattern of land surface temperatures, land cover and neighborhood socioeconomic characteristics in Baltimore, MD, *J. Environ. Manage.*, *92*(7), 1753–1759, doi:10.1016/j.jenvman.2011.02.006.
Hughes, S., S. Pincetl, and C. Boone (2013), Triple exposure: Regulatory, climatic, and political drivers of water management changes in the city of Los Angeles, *Cities*, *32*(June), 51–59, doi:10.1016/j.cities.2013.02.007.
Jenerette, G. D., S. L. Harlan, A. Brazel, N. Jones, L. Larsen, and W. L. Stefanov (2007), Regional relationships between surface temperature, vegetation, and human settlement in a rapidly urbanizing ecosystem, *Landscape Ecol.*, *22*, 353–365, doi:10.1007/s10980-006-9032-z.
Jenerette, G. D., S. L. Harlan, W. L. Stefanov, and C. A. Martin (2011), Ecosystem services and urban heat riskscape moderation: Water, green spaces, and social inequality in Phoenix, USA, *Ecol. Appl.*, *21*(7), 2637–51.
Jenerette, G. D., et al. (2016), Climate tolerances and trait choices shape continental patterns of urban tree biodiversity, *Glob. Ecol. Biogeogr.*, *25*, 1367–1376, doi:10.1111/geb.12499.
Koster, R. D., and M. J. Suarez (1994), The components of a "SVAT" scheme and their effects on a GCM's hydrological cycle, *Adv. Water Resour.*, *17*(1–2), 61–78, doi:10.1016/0309-1708(94)90024-8.
Koster, R. D., and M. J. Suarez (1996), *Energy and Water Balance Calculations in the Mosaic LSM*, Greenbelt, Md.
Kumar, S. V., et al. (2006), Land information system: An interoperable framework for high resolution land surface modeling, *Environ. Model. Softw.*, *21*(10), 1402–1415, doi:10.1016/j.envsoft.2005.07.004.
LADWP (2016a), *2016 Briefing Book. Water System*, Los Angeles Dep. of Water and Power, Los Angeles, Calif.
LADWP (2016b), *Emergency Water Conservation Plan Ordinance*, Los Angeles Dep. of Water and Power, Los Angeles, Calif.
Larcher, W. (2001), *Physiological Plant Ecology*, 4th ed., Verlag Eugen Ulmer, Stuttgart, Germany.
Liang, X., D. P. Lettenmaier, E. F. Wood, and S. J. Burges (1994), A simple hydrologically based model of land surface water and energy fluxes for general circulation models, *J. Geophys. Res.*, *99*(D7), 14,415, doi:10.1029/94JD00483.
Litvak, E., and D. E. Pataki (2016), Evapotranspiration of urban lawns in a semi-arid environment: An *in situ* evaluation of microclimatic conditions and watering recommendations, *J. Arid Environ.*, *134*, 87–96.
Litvak, E., H. R. McCarthy, and D. E. Pataki (2011), Water relations of coast redwood planted in the semi-arid climate of southern California, *Plant. Cell Environ.*, *34*(8), 1384–400, doi:10.1111/j.1365-3040.2011.02339.x.
Litvak, E., H. R. McCarthy, and D. E. Pataki (2012), Transpiration sensitivity of urban trees in a semi-arid climate is constrained by xylem vulnerability to cavitation, *Tree Physiol.*, *32*, 373–388, doi:10.1093/treephys/tps015.
Litvak, E., N. S. Bijoor, and D. E. Pataki (2014), Adding trees to irrigated turfgrass lawns may be a water-saving measure in semi-arid environments, *Ecohydrology*, *7*(5), 1314–1330, doi:10.1002/eco.1458.
Litvak, E., H. R. Mccarthy, and D. E. Pataki (2017), A method for estimating transpiration of irrigated urban trees in California, *Landscape Urban Plann.*, *158*, 48–61, doi:10.1016/j.landurbplan.2016.09.021.
Long, D., and V. P. Singh (2013), Assessing the impact of end-member selection on the accuracy of satellite-based spatial variability models for actual evapotranspiration estimation, *Water Resour. Res.*, *49*, 2601–2618, doi:10.1002/wrcr.20208.
Long, D., L. Longuevergne, and B. R. Scanlon (2014), Uncertainty in evapotranspiration fromland surfacemodeling, remote sensing, and GRACE satellites, *Water Resour. Res.*, *50*, 1131–1151, doi:10.1002/2013WR014581.Received.
MacDonald, G. M. (2010), Water, climate change, and sustainability in the southwest, *Proc. Natl. Acad. Sci. U. S. A.*, *107*(50), 21,256–21,262, doi:10.1073/pnas.0909651107.
Mahrt, L., and M. Ek (1984), The influence of atmospheric stability on potential evaporation, *J. Clim. Appl. Meteorol.*, *23*, 222–234, doi:10.1175/1520-0450(1984)023<0222:TIOASO>2.0.CO;2.
McCarthy, H. R., and D. E. Pataki (2010), Drivers of variability in water use of native and non-native urban trees in the greater Los Angeles area, *Urban Ecosyst.*, *13*(4), 393–414, doi:10.1007/s11252-010-0127-6.
McPherson, E. G., J. R. Simpson, Q. Xiao, and C. Wu (2008), *Los Angeles 1-Million Tree Canopy Cover Assessment. General Tachnical Report PSW-GTR-207*, U.S. Dep. of Agric., For. Serv., Pac. Southwest Res. Stn.
McPherson, E. G., J. R. Simpson, Q. Xiao, and C. Wu (2011), Million trees Los Angeles canopy cover and benefit assessment, *Landscape Urban Plann.*, *99*(1), 40–50, doi:10.1016/j.landurbplan.2010.08.011.
Melillo, J. M., T. C. Richmond, and G. W. Yohe (Eds.) (2014), *Climate Change Impacts in the United States: The Third National Climate Assessment*, U.S. Global Change Res. Prog., Washington, D. C.

Mini, C., T. S. Hogue, and S. Pincetl (2014), Estimation of residential outdoor water use in Los Angeles, California, *Landscape Urban Plann.*, *127*, 124–135, doi:10.1016/j.landurbplan.2014.04.007.
Mitchell, K. E., et al. (2004), The multi-institution North American Land Data Assimilation System (NLDAS): Utilizing multiple GCIP products and partners in a continental distributed hydrological modeling system, *J. Geophys. Res.*, *109*, D07S90, doi:10.1029/2003JD003823.
Monaghan, A. J., L. Hu, N. A. Brunsell, M. Barlage, and O. V. Wilhelmi (2014), Evaluating the impact of urban morphology configurations on the accuracy of urban canopy model temperature simulations with MODIS, *J. Geophys. Res. Atmos.*, *119*, 6376–6392, doi:10.1002/2013JD021227.
Monteith, J. L. (1965), Evaporation and environment, *Symosia Soc. Exp. Biol.*, *19*, 205–234.
Mu, Q., M. Zhao, and S. W. Running (2011), Improvements to a MODIS global terrestrial evapotranspiration algorithm, *Remote Sens. Environ.*, *115*(8), 1781–1800, doi:10.1016/j.rse.2011.02.019.
Nishida, K., R. R. Nemani, S. W. Running, and J. M. Glassy (2003), An operational remote sensing algorithm of land surface evaporation, *J. Geophys. Res.*, *108*(D9), 4270, doi:10.1029/2002JD002062.
Nordbo, A., L. Järvi, and T. Vesala (2012), Revised eddy covariance flux calculation methodologies—Effect on urban energy balance, *Tellus, Ser. B*, *64*, 18,184, doi:10.3402/tellusb.v64i0.18184.
Nouri, H., S. Beecham, F. Kazemi, and A. M. Hassanli (2013), A review of ET measurement techniques for estimating the water requirements of urban landscape vegetation, *Urban Water J.*, *10*(4), 247–259, doi:10.1080/1573062X.2012.726360.
Nouri, H., E. Glenn, S. Beecham, S. Chavoshi Boroujeni, P. Sutton, S. Alaghmand, B. Noori, and P. Nagler (2016), Comparing three approaches of evapotranspiration estimation in mixed urban vegetation: Field-based, remote sensing-based and observational-based methods, *Remote Sens.*, *8*(6), 492, doi:10.3390/rs8060492.
Nowak, D. J., R. E. I. Hoehn, D. E. Crane, L. Weller, and A. Davila (2010), *Assessing Urban Forest Effects and Values*, Los Angeles Urban For., USDA For. Serv., Delaware, Ohio.
Offerle, B., C. S. B. Grimmond, K. Fortuniak, and W. Pawlak (2006), Intraurban differences of surface energy fluxes in a Central European City, *J. Appl. Meteorol. Climatol.*, *45*(1), 125–136, doi:10.1175/JAM2319.1.
Oke, T. R. (1979), Advectively-assisted evapotranspiration from irrigated urban vegetation, *Boundary Layer Meteorol.*, *17*(2), 167–173.
Pataki, D. E., C. G. Boone, and T. S. Hogue (2011a), Socio-ecohydrology and the urban water challenge, *Ecohydrology*, *347*, 341–347, doi:10.1002/eco.209.
Pataki, D. E., H. R. McCarthy, E. Litvak, and S. Pincetl (2011b), Transpiration of urban forests in the Los Angeles metropolitan area., *Ecol. Appl.*, *21*(3), 661–677.
Pataki, D. E., H. R. McCarthy, T. Gillespie, and G. D. Generette (2013), A trait-based ecology of the Los Angeles urban forest, *Ecosphere*, *4*(6), 1–20, doi:10.1890/ES13-00017.1.
Penman, H. (1948), Natural evaporation from open water, bare soil and grass, *Proc. R. Soc. Lond. A*, *193*(1032), 120–145.
Pereira, L. S., and A. Perrier (1999), Evapotranspiration: Concepts and future trends, *J. Irrig. Drain. Eng.*, *125*(2), 45–51.
Pereira, L. S., R. G. Allen, M. Smith, and D. Raes (2015), Crop evapotranspiration estimation with FAO56: Past and future, *Agric. Water Manage.*, *147*, 4–20, doi:10.1016/j.agwat.2014.07.031.
Peters, E. B., R. V. Hiller, and J. P. McFadden (2011), Seasonal contributions of vegetation types to suburban evapotranspiration, *J. Geophys. Res.*, *116*, G01003, doi:10.1029/2010JG001463.
Pincetl, S., E. Porse, and D. Cheng (2016), Fragmented flows: Water supply in Los Angeles County, *Environ. Manage.*, *58*(2), 208–222.
Pittenger, D. R., and D. A. Shaw (2007), Review of research on water needs of landscape plants, in *Symposium on Efficient Water Use in the Urban Landscape*, New Mexico State Univ., Las Cruces, N. M.
Pittenger, D. R., and D. A. Shaw (2010), Estimating water needs of urban landscapes, in *Annual Conference of the American Society for Horticultural Science, Supplement to HortScience 45(8)*, S95, Palm Desert, Calif. [Available online at http://hortsci.ashspublications.org/content/suppl/2010/08/16/45.8.DC1/HortScienceVol45-8supplement.pdf.]
Pittenger, D. R., A. James Downer, D. R. Hodel, and M. Mochizuki (2009), Estimating water needs of landscape palms in mediterranean climates, *Horttechnology*, *19*(4), 700–704.
Potchter, O., D. Goldman, D. Kadish, and D. Iluz (2008), The oasis effect in an extremely hot and arid climate: The case of southern Israel, *J. Arid Environ.*, *72*, 1721–1733, doi:10.1016/j.jaridenv.2008.03.004.
Rahman, M., and R. Ennos (2016), *What We Know and Don't Know About the Cooling Benefits of Urban Trees*, Technical Report, Trees & Design Action Group, www.tdag.org.uk/research.html, doi:10.13140/RG.2.1.5122.2645.
Rahman, M. A., A. Moser, T. Roetzer, and S. Pauleit (2017), Microclimatic differences and their influence on transpirational cooling of Tilia cordata in two contrasting street canyons in Munich, Germany, *Agric. For. Meteorol.*, *232*, 443–456, doi:10.1016/j.agrformet.2016.10.006.
Renninger, H. J., N. Phillips, and D. R. Hodel (2009), Comparative hydraulic and anatomic properties in palm trees (*Washingtonia Robusta*) of varying heights: Implications for hydraulic limitation to increased height growth, *Trees*, *23*(5), 911–921, doi:10.1007/s00468-009-0333-0.
Roth, M. (2000), Review of atmospheric turbulence over cities, *Q. J. R. Meteorol. Soc.*, *126*(564), 941–990, doi:10.1002/qj.49712656409.
Sabo, J. L., et al. (2010), Reclaiming freshwater sustainability in the Cadillac Desert, *Proc. Natl. Acad. Sci. U. S. A.*, *107*(50), 21,263–21,270, doi:10.1073/pnas.1009734108.
Sanders, K. T. (2016), The energy trade-offs of adapting to a water-scarce future: Case study of Los Angeles, *Int. J. Water Resour. Dev.*, *32*(3), 362–378, doi:10.1080/07900627.2015.1095079.
Schmid, H. P. (2002), Footprint modeling for vegetation atmosphere exchange studies: A review and perspective, *Agric. For. Meteorol.*, *113*(1–4), 159–183, doi:10.1016/S0168-1923(02)00107-7.
Shashua-Bar, L., D. Pearlmutter, and E. Erell (2009), The cooling efficiency of urban landscape strategies in a hot dry climate, *Landscape Urban Plann.*, *92*(3–4), 179–186, doi:10.1016/j.landurbplan.2009.04.005.
Shashua-Bar, L., D. Pearlmutter, and E. Erell (2011), The influence of trees and grass on outdoor thermal comfort in a hot-arid environment, *Int. J. Climatol.*, *31*(10), 1498–1506, doi:10.1002/joc.2177.
Shields, C. A., and C. L. Tague (2012), Assessing the role of parameter and input uncertainty in ecohydrologic modeling: Implications for a semi-arid and urbanizing coastal California catchment, *Ecosystems*, *15*, 775–791, doi:10.1007/s10021-012-9545-z.
Simpson, J. R. (2002), Improved estimates of tree-shade effects on residential energy use, *Energy Buildings*, *34*(10), 1067–1076, doi:10.1016/S0378-7788(02)00028-2.
Spano, D., R. L. Snyder, C. Sirca, and P. Duce (2009), ECOWAT-A model for ecosystem evapotranspiration estimation, *Agric. For. Meteorol.*, *149*(10), 1584–1596, doi:10.1016/j.agrformet.2009.04.011.
Steinwand, A. L., R. F. Harrington, and D. Or (2006), Water balance for Great Basin phreatophytes derived from eddy covariance, soil water, and water table measurements, *J. Hydrol.*, *329*(3–4), 595–605, doi:10.1016/j.jhydrol.2006.03.013.
St. Hilaire, R., et al. (2008), Efficient water use in residential urban landscapes, *HortScience*, *43*(7), 2081–2092.

Sun, H., K. Kopp, and R. Kjelgren (2012), Water-efficient urban landscapes: Integrating different water use categorizations and plant types, *HortScience*, *47*(2), 254–263.
Tayyebi, A., and D. G. Jenerette (2016), Increases in the climate change adaption effectiveness and availability of vegetation across a coastal to desert climate gradient in metropolitan Los Angeles, CA, USA, *Sci. Total Environ.*, *548 549–*, 60–71, doi:10.1016/j.scitotenv.2016.01.049.
Thom, J. K., A. M. Coutts, A. M. Broadbent, and N. J. Tapper (2016), The influence of increasing tree cover on mean radiant temperature across a mixed development suburb in Adelaide, Australia, *Urban For. Urban Green.*, doi:10.1016/j.ufug.2016.08.016.
Thornberg, C., J. Levine, R. De Anda, A. Hooper, and V. Pike Bond (2015), *Los Angeles City Council Districts Economic Report 2015*, Beacon Economics, Los Angeles, Calif. [Available at http://www.lachamber.com/clientuploads/policy_issues/15_BeaconReport_Web.pdf.]
Troy, T. J., E. F. Wood, and J. Sheffield (2008), An efficient calibration method for continental-scale land surface modeling, *Water Resour. Res.*, *44*, W09411, doi:10.1029/2007WR006513.
Vahmani, P., and T. S. Hogue (2014a), High-resolution land surface modeling utilizing remote sensing parameters and the Noah UCM: A case study in the Los Angeles Basin, *Hydrol. Earth Syst. Sci.*, *18*(12), 4791–4806, doi:10.5194/hess-18-4791-2014.
Vahmani, P., and T. S. Hogue (2014b), Incorporating an urban irrigation module into the Noah land surface model coupled with an urban canopy model, *J. Hydrometeorol.*, *15*, 1440–1456, doi:10.1175/JHM-D-13-0121.1.
Vahmani, P., and T. S. Hogue (2015), Urban irrigation effects on WRF-UCM summertime forecast skill over the Los Angeles metropolitan area, *J. Geophys. Res. Atmos.*, *120*, 9869–9881, doi:10.1002/2015JD023239.
Wang, C., J. Yang, S. W. Myint, Z.-H. Wang, and B. Tong (2016a), Empirical modeling and spatio-temporal patterns of urban evapotranspiration for the Phoenix metropolitan area, Arizona, *GISci. Remote Sens.*, *53*(6), 778–792, doi:10.1080/15481603.2016.1243399.
Wang, Z. H., X. Zhao, J. Yang, and J. Song (2016b), Cooling and energy saving potentials of shade trees and urban lawns in a desert city, *Appl. Energy*, *161*, 437–444.
Wei, H., Y. Xia, K. E. Mitchell, and M. B. Ek (2013), Improvement of the Noah land surface model for warm season processes: Evaluation of water and energy flux simulation, *Hydrol. Processes*, *27*(2), 297–303, doi:10.1002/hyp.9214.
Xie, J., et al. (2016), Seasonal variation in ecosystem water use efficiency in an urban-forest reserve affected by periodic drought, *Agric. For. Meteorol.*, *221*, 142–151, doi:10.1016/j.agrformet.2016.02.013.
Yang, J., and Z. H. Wang (2015), Optimizing urban irrigation schemes for the trade-off between energy and water consumption, *Energy Buildings*, *107*, 335–344, doi:10.1016/j.enbuild.2015.08.045.
Yang, Y., D. Long, and S. Shang (2013), Remote estimation of terrestrial evapotranspiration without using meteorological data, *Geophys. Res. Lett.*, *40*, 3026–3030, doi:10.1002/grl.50450.
Zhang, K., J. S. Kimball, R. R. Nemani, and S. W. Running (2010), A continuous satellite-derived global record of land surface evapotranspiration from 1983 to 2006, *Water Resour. Res.*, *46*, W09522, doi:10.1029/2009WR008800.
Zipper, S. C., J. Schatz, C. J. Kucharik, and S. P. Loheide (2017), Urban heat island-induced increases in evapotranspirative demand, *Geophys. Res. Lett.*, *44*, 873–881, doi:10.1002/2016GL072190.